RSC Advances

PAPER

View Article Online
View Journal | View Issue

Cite this: *RSC Adv.*, 2018, **8**, 2365

A facile molecularly imprinted polymer-based fluorometric assay for detection of histamine

Xiaotong Feng, Jon Ashley, Tongchang Zhou, Arnab Halder and Yi Sun *

Histamine is a biogenic amine naturally present in many body cells. It is also a contaminant that is mostly found in spoiled food. The consumption of foods containing high levels of histamine may lead to an allergy-like food poisoning. Analytical methods that can routinely screen histamine are thus urgently needed. In this paper, we developed a facile and cost-effective molecularly imprinted polymer (MIP)-based fluorometric assay to directly quantify histamine. Histamine-specific MIP nanoparticles (nanoMIPs) were synthesized using a modified solid-phase synthesis method. They were then immobilized in the wells of a microplate to bind the histamine in aqueous samples. After binding, *o*-phthaldialdehyde (OPA) was used to label the bound histamine, which converted the binding events into fluorescent signals. The obtained calibration curve of histamine showed a linear correlation ranging from 1.80 to 44.98 μM with the limit of detection of 1.80 μM. This method was successfully used to detect histamine in spiked diary milk with a recovery rate of more than 85%.

Received 18th October 2017
Accepted 1st January 2018

DOI: 10.1039/c7ra11507e

rsc.li/rsc-advances

1. Introduction

Histamine is a biogenic amine that is involved in the immune response and regulation of physiological functions.[1,2] High levels of histamine have been widely found in a number of food sources including fish, pork, spinach, cheese and nuts,[3] which can trigger an intolerance within individuals, leading to symptoms such as itchy eyes, runny nose, congestion, asthma, eczema, hot flushes, migraines and in extreme cases death from anaphylactic shock.[1,4] According to EU legislation, the maximum residual limit (MRL) of histamine is 2–20 mg L^{-1} in beverages and 50–100 mg kg^{-1} in fermented food.[5,6] Therefore, monitoring the level of histamine in food is very important for food safety control.

Currently, thin layer chromatography (TLC),[7] gas chromatography (GC),[8] high performance liquid chromatography (HPLC)[9] and capillary zone electrophoresis (CZE)[10] are among the most commonly used analytical methods to detect histamine. Although the sensitivity of these methods is high, they often require expensive, sophisticated instrumentation, as well as time-consuming sample preparation. Alternatively, colorimetric[11] and enzyme-linked immunosorbent assay (ELISA)[12] are the most commonly used methods for preliminary screening. These commercially available kits rely on either a dehydrogenase enzyme to catalyze oxidation of histamine or an antibody to selectively bind histamine and form tight complexes. Although the enzyme and antibody possess high specificity and affinity, these bioreceptors are expensive and inherently unstable due to the biological origins.

To overcome the limitations of natural receptors, great attention has been paid to develop biomimetic receptors using molecularly imprinted polymers (MIPs).[13,14] The technique involves the formation of binding sites in a synthetic polymer matrix that are of a complementary functional and structural character to its "substrate" molecule. MIPs have been synthesized for diverse food relevant analytes ranging from small molecules to big proteins and pathogens. Attributed to their thermal stability, robustness and low cost, these so called "plastic antibodies" have shown great potential for use in bioassays.[15,16] Molecular imprinting of histamine has been reported earlier.[17–19] However, these histamine MIPs suffered from different drawbacks as they were synthesized mainly by bulk polymerization or precipitation polymerization. For bulk polymerization, the resultant MIP particles often display large size variations due to the formation of the monolith followed by grinding. Moreover, it is challenging to completely remove the residual templates in the MIPs.[20] Precipitation polymerization is a simple one-step polymerization which results in nanoparticles with a narrower size distribution.[21] However, the template, monomers and crosslinker need to be dissolved into the porogen solvent with high dilution factor, resulting in negative impact on the interaction between the monomers and the template. Additionally, both methods give high binding site heterogeneity (highly polyclonal), which can lead to high levels of non-specific binding.

To address the drawbacks of bulk polymerization and precipitation polymerization, Canfarotta *et al.* proposed a solid-phase approach to synthesize nano-sized MIPs (nanoMIPs) by

Department of Micro- and Nanotechnology, Technical University of Denmark, Ørsteds Plads, DK-2800 Kgs, Lyngby, Denmark. E-mail: Sun.Yi@nanotech.dtu.dk; Tel: +45 4525 6319

attaching the analyte onto glass beads.[22] These nanoparticles could be quickly formed and removed from the template without further purification, and nanoMIPs with uniform size and high binding site homogeneity were achieved. Solid-phase synthesis has been used to imprint molecules such as melamine, vancomycin and trypsin, and showed great promise for both small molecules and proteins.

Besides the synthesis of MIPs, another challenge associated with developing MIP-based assay is the signal transduction. Since MIPs usually contain no inherent signaling element, it is difficult to transform the binding events into measurable optical or electronic signals. So far, the MIPs have been used together with surface enhanced Raman spectroscopy,[17] voltammetric sensor[18] and UV-vis spectrometry[19] for detection of histamine, but these methods are not suitable for routine high-throughput screening purpose. Recently, a so called "Pseudo-ELISA"[23–26] has been developed, where the nanoMIPs were used as replace natural antibodies in ELISA. In the assay, the nanoMIPs were immobilized in a microplate, and the analyte was quantified through the competitive binding between the free analyte and horseradish peroxidase-conjugated analyte. Though the pseudo-ELISA was promising for high-throughput screening, it required pre-conjugation of analyte with the enzyme, as well as several rounds of blocking, incubation and washing steps, which made the assay costly and time-consuming.

In this work, we developed a new MIP-based fluorometric assay for the rapid detection of histamine in food samples. Histamine nanoMIPs were synthesized using the modified solid-phase synthesis (Fig. 1). The binding affinity of the nanoMIPs with histamine was determined to be 0.89 nM, similar to anti-histamine antibody. A simple and cost-effective bioassay using histamine nanoMIPs as artificial receptor was then developed. The concept is shown in Fig. 2. The nanoMIPs were immobilized in a 96-well microplate by physical absorption, and samples with different concentrations of histamine were added to the wells. After incubation for a short period, the wells were washed. Subsequently, *o*-phthaldialdehyde (OPA) solution which can react specifically with primary amines[27] was added to the wells to label the bound histamine, and the fluorescent intensity at 440 nm was recorded and used for quantification. Unlike the pseudo-ELISA approach, there is no need to prepare pre-labeled analyte in this assay. Instead of the long incubation time and multiple steps needed to develop color with horseradish peroxidase, it only took 4 min for OPA to give fluorescence signal. The feasibility of using the newly developed assay to detect histamine in food matrices, such as dairy milk, was successfully demonstrated. A limit detection of 1.80 μM and a recovery rate of more than 85% were achieved. To our best knowledge, this is the first time that nanoMIP-based OPA fluorometric assay is reported.

2. Experimental

2.1. Materials

Methacrylic acid (MAA), ethylene glycol dimethacrylate (EGDMA), trimethylolpropane trimethacrylate (TRIM), pentaerythritol-tetrakis-(3-mercaptopropionate) (PETMP), phosphate buffer solution (PBS) (pH 7.4), sodium hydroxide, glutaraldehyde (GA), histamine, histidine, melamine, (3-aminopropyl)triethoxysilane (APTES). Carbodiimide (EDC), *N*-hydroxysuccinimide (NHS) 98%, ethanolamine hydrochloride, hydrochloride acid (HCl), 11-mercaptoundecanoic acid (MUDA) 95%, hydrogen peroxide, acetonitrile (ACN), ethanol, acetone, phthaldialdehyde, 60 mL SPE tubes and 20 μm pore frits and glass beads (75 μm), were purchased from Sigma-Aldrich (DK). 2,4,6-Trinitrobenzene sulfonic acid (TNBSA) was purchased from Thermofisher Scientific (DK). *N*,*N*-Diethyldithiocarbamic acid benzyl ester (DABE) was obtained from TCI Europe (Belgium). Q-Max® Celluloseacetat (CA) syringe filters 0.45 μm were from FRISENETTE (DK). Gold chip was purchased from Bionavis, Sweden. Nunclon 96-well flat-bottom black microwell plates were purchased from Thermo scientific, DK. 0.1% milk (Arla) was bought from a local supermarket, Netto. Deionized water was obtained from a Millipore (MilliQ) purification system. All chemicals were analytical or HPLC grade and were used without further purification.

2.2. Synthesis of histamine nanoMIPs

As shown in Fig. 1, the histamine nanoMIPs was synthesized by solid-phase approach. The protocol was adapted from the method developed by Canfarotta *et al.*[22]

Preparation of template-derivatised glass beads. Histamine was firstly immobilized covalently onto glass beads (Fig. 1a). Ten grams of glass beads were activated by boiling in 20 mL 4 M NaOH solution for 15 min, thoroughly rinsed with MilliQ water and acetone, and then dried in an oven at 80 °C. To introduce amino groups to the surface of the glass beads, the dry beads were incubated overnight in 20 mL of 2% v/v APTES/toluene solution and then washed with acetone and methanol. The presence of the amino groups was determined by incubation of a small aliquot of the glass beads with TNBSA reagent. Next, the incubated glass beads were mixed with 20 mL of 5% v/v GA in PBS at pH 7.2 for 2 h at 25 °C to form Schiff base bonds. Ten milliliters of histamine in PBS (5 mg mL^{-1}) was added to glass beads and incubated overnight at 4 °C to immobilize histamine on the glass beads. Afterwards, unbound histamine was washed away from glass beads by using MilliQ water and incubated with 20 mL 1 mg mL^{-1} $NaBH_4$ to reduce the Schiff base bonds on the glass beads. Finally, the glass beads were washed with MilliQ water, dried under vacuum and stored at 4 °C.

Synthesis of histamine nanoMIPs. The polymerization mixture for synthesizing histamine nanoMIPs was prepared by mixing 6.69 μmol of MAA as the functional monomer, 3.27 μmol of EGDMA and 1.91 μmol of TRIM as the cross-linkers, 0.62 μmol of *N*,*N*-diethyldithiocarbamic acid benzyl ester as the iniferter photoinitiator and 0.07 μmol of pentaerythritol-tetrakis-(3-mercaptopropionate) (CTA) as the chain transfer agent (Fig. 1b). The interaction between histamine and MAA is illustrated in Fig. 1c. All the compounds were dissolved into 2.67 mL ACN in a glass vial and purged with nitrogen for 30 min. Ten grams of histamine-derivatised glass beads was placed in a 200 mL flat-bottomed glass beaker and degassed

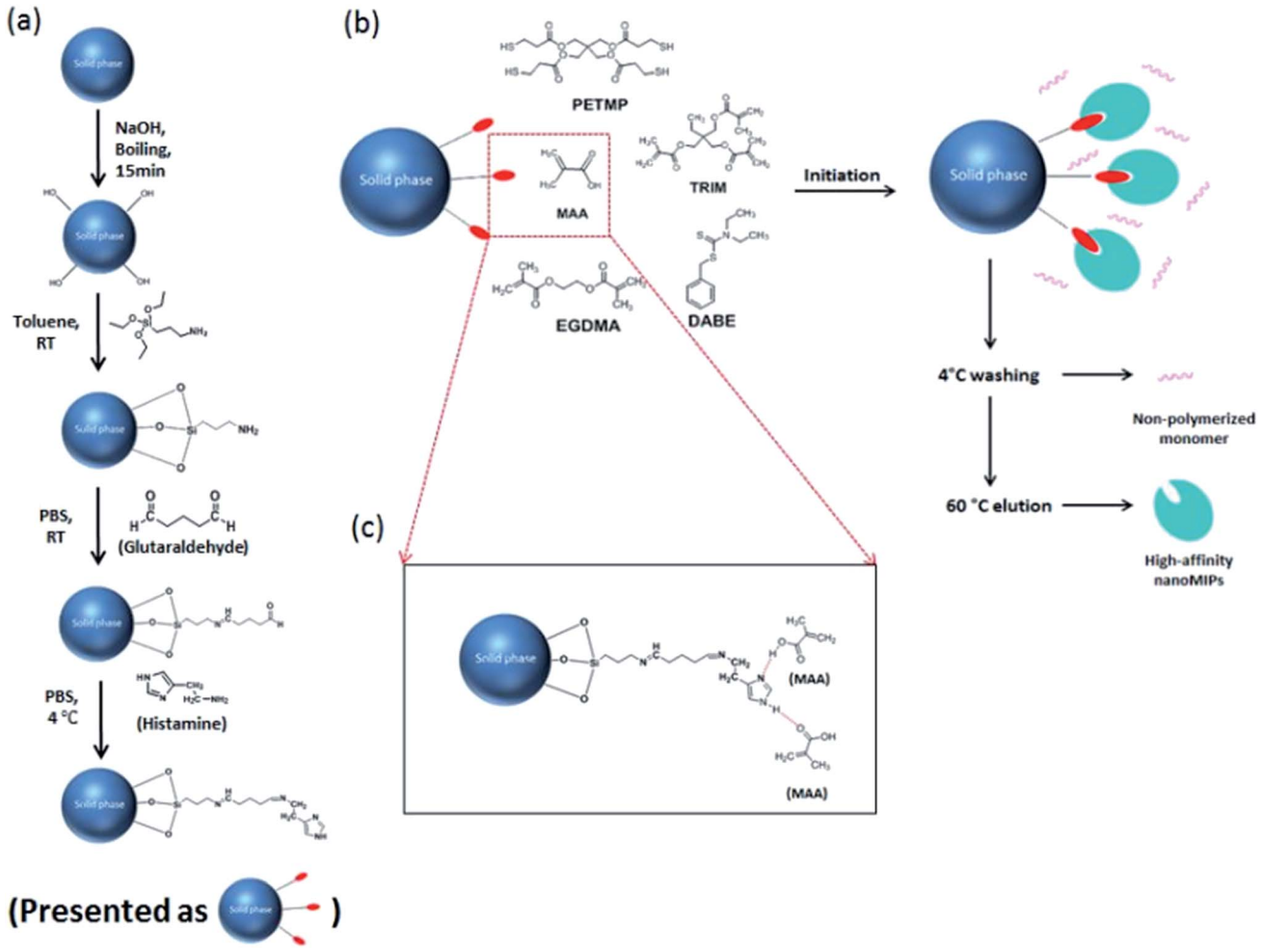

Fig. 1 (a) Immobilization of histamine on the surface of glass beads. (b) Solid phase synthesis of histamine nanoMIPs. (c) Interaction between immobilized histamine and functional monomer MAA.

under vacuum for 30 min. The polymerization mixture was poured onto the glass beads and then the beaker was placed into a custom-made photoreactor fitted with 16 UV bubbles (8.3 W each). The photopolymerization was initiated by exposing the reaction mixture to UV light for 10–30 seconds at room temperature. After polymerization, all the content was transferred into a solid phase extraction (SPE) cartridge (60 mL syringe tube) fitted with polyethylene frit (20 μm porosity), and was washed using 15 bed volumes of ACN at 4 °C to remove non-polymerized monomers. Next, 60 °C ACN was poured in to the cartridge and incubated with histamine-derivatised glass beads for 15 min in a 60 °C water bath. This procedure was performed several times to allow the elution of high affinity nanoMIPs from the solid phase. The total eluted volume was about 50 mL. Finally, glass beads were washed by 50 mL of 0.01 M HCl and 50 mL of MilliQ water at 60 °C for reuse.

2.3. Characterization of nanoMIPs

The yields of histamine nanoMIPs were measured by calculating the weight yield value from a 10 mL aliquot of nanoMIPs solution. In general, 10 mL of stock solution (in ACN) was evaporated under a stream of nitrogen in a pre-weighed empty vial. After evaporating, the glass vial was put into a vacuum oven at 80 °C for overnight.

Nanoparticle size and quality were determined by dynamic light scattering (DLS) using a NanoBrook ZetaPALS Potential Analyzer (Brookhaven, USA). Ten milliliters of stock solution (in ACN) was evaporated under a stream of nitrogen. Two milliliters of MilliQ water was added and sonicated for 20 min. The dispersion was filtered through a 0.45 μm CA syringe filter to remove dust and possible aggregates. The filtered histamine nanoMIPs were analyzed by DLS at 25 °C in a 3 cm^3 disposable polystyrene cuvette. The values were reported as an average of 5 measurements.

Scanning electron microscopy (SEM) analysis was carried out on a Quanta FEG 200 ESEM scanning electron microscopy (FEI). Five milliliters of stock solution (in ACN) was subjected to evaporation and replacement by 0.5 mL MilliQ water. The solution was sonicated for 20 min followed by filtering through a 0.45 μm CA syringe filter. A drop of histamine nanoMIPs was placed on a silica wafer and dried in a desiccator overnight. Prior to SEM, the sample was sputtered with a thin layer of gold using a Quorum Coater.

Fig. 2 NanoMIP-based OPA fluorometric assay for detection of histamine.

2.4. Surface plasma resonance (SPR)

Prior to SPR analysis, 25 mL of histamine nanoMIP stock solution was evaporated using a stream of nitrogen, 2 mL of PBS was added followed by 30 min of sonication. Aqueous stock suspensions of the histamine MIPs were filtered through CA syringe filters with 0.45 μm pore size and diluted in PBS for analysis followed by a series of 2× dilutions. Apparent molarity of nanoMIPs was calculated by approximating nanoMIPs as regular spheres, and the concentration of the nanoMIP was determined from the following equation.[28]

$$[\mathrm{NP}] = \frac{6}{\pi N_A d^3 \rho} X \quad (1)$$

where N_A is Avogadro's constant, d is the hydrodynamic diameter of particles measured by DLS (nm), ρ is polymer density of particles (g cm^{-3}) and X is the weight concentration (mg mL^{-1}) of stock solution.

SPR experiments were performed on a MP-SPR Navi™ 200 OTSO (Bionavis, Sweden). Au-coated chips were cleaned in Piranha solution (H_2SO_4 : H_2O_2, 3 : 1 v/v) for 5 min, and rinsed with MilliQ water. For immobilization of histamine, cleaned chips were dried under N_2 and placed in a solution of 5 mM MUDA at 4 °C overnight to form a self-assembled layer (SAM). The resultant gold chip was promptly washed with water and ethanol, dried under nitrogen. The chip was docked in the MP-SPR Navi™ 200 OTSO and 10 mM PBS was pumped through the flow cell. The instrument was primed at a flow rate of 20 μL min^{-1}. Upon obtaining a stable baseline, a mixture containing 100 μL 0.4 M EDC and 0.1 M NHS (100 μL) was injected followed by an injection of histamine (100 μL). Any remaining NHS ester groups were deactivated by injecting 1 M ethanolamine HCl (100 μL) in ethanol at a flow rate of 20 μL min^{-1}. Hundred microliters of histamine nanoMIPs (0.05 nM to 5 nM) were injected sequentially over the immobilized histamine from the lowest to highest concentration, the responses were recorded and the signal from the reference channel was subtracted. The binding affinity dissociation constants (K_D) were calculated from Advanced Analysis Software TraceDrawer™ by 1 : 1 binding model with drifting baseline fitting.

2.5. UV/vis binding assay

Binding properties of the synthesized nanoMIPs were tested in UV spectrophotometric analysis in PBS buffer. One milliliter of histamine nanoMIPs (5 mg mL^{-1}) was mixed with 10 μL of various concentrations of histamine in glass vials followed by shaking for 20 h at room temperature. The used concentrations of histamine were 5 mg mL^{-1}, 2.5 mg mL^{-1} and 1.25 mg mL^{-1}, respectively. The same procedure was applied to histidine and melamine. After incubation, the solutions were centrifuged at 15 000*g* for 30 min and the supernatant was collected (500 μL). The concentration of free analyte was measured by UV-2600 UV-vis spectrophotometer (Holm&Halby, Denmark). The absorbance maxima wavelength for UV/vis detection of histamine, histidine and melamine were 209 nm, 210 nm and 204 nm, respectively.

2.6. Development of OPA fluorometric assay for histamine detection

Fifty microliters of histamine nanoMIPs (2 μg μL^{-1}) were dispensed into each well of Nunclon 96-well flat-bottom black

microplate, and left to dry completely overnight at room temperature in the fume hood. To remove the unattached histamine nanoMIPs, 100 μL of 10 mM PBS was used to wash the well plate three times. Next, a series dilution of 100 μL histamine from 1.8 μM to 1799.4 μM was dispensed into the wells and incubated for 4 h. After incubation, histamine was removed and the plate was washed three times using 100 μL PBS. To each well, 90 μL of 0.1 M HCl was added followed by adding 18 μL of 1 M NaOH and 4.5 μL of OPA (in ethanol). Histamine was allowed to react with OPA in a dark room at room temperature for 4 min and the reaction was stopped by adding 9 μL of 3 M HCl. Finally, the fluorescence spectra were measured from 400 to 600 nm at an excitation wavelength of 360 nm, using a Spark® multimode microplate reader (Tecan, Sweden). The fluorescent intensity at 440 nm was used to build the calibration curve.

Optimization of incubation time. For the optimization of incubation time, microplates were prepared as described above using 2 μg mL^{-1} of histamine for each incubation mixture. Besides incubating the nanoMIPs with histamine overnight, different incubation times of 5 min, 10 min, 30 min, 1 h, 2 h and 4 h, were also tested.

2.7. Analysis of histamine in milk

0.1% milk (Arla) was diluted 10 folds by MilliQ water. The histamine with the concentrations of 0 μM, 4.5 μM, 13.5 μM, 27 μM and 40.48 μM was spiked into the milk. Histamine spiked milk was incubated into each nanoMIP-immobilized well for 4 h followed by washing using PBS for three times. OPA fluorometric assay was performed as described in Section 2.6. The concentration of histamine in the diluted milk was derived from the calibration curve.

3. Results and discussion

3.1. Characterization of histamine nanoMIPs

With the solid-phase synthesis approach, nanoMIPs were produced within just a few minutes (depending on the power of UV sources). Furthermore, unlike in traditional methods such as suspension polymerization where 3 day-dialysis is required to remove the template, the nanoMIPs can be easily removed from the template since the binding sites are in the surface of nanoparticles.

The nanoMIPs were synthesized *via* a UV-initiated living polymerization mechanism. Iniferter (initiator, transfer agent, terminator) was used instead of initiator because it allowed for a better control of polymer chain growing, thereby resulting in narrower molecular weight distribution of resultant polymers as compared to conventional free radical initiators.[29] Since a custom-made light-tight UV photo reactor was used, the effect of UV exposure time on the properties of nanoMIPs was investigated. The photopolymerization was carried out at 10 s, 20 s, and 30 s, respectively. The size, yield and apparent dissociation constant K_D of histamine nanoMIPs are summarized in Table 1. The results showed that there was a direct correlation between exposure time, yield and the size of the nanoMIPs produced. For instance, by increasing the exposure time from 10 s to 30 s, the yield of the nanoMIPs increased from 0.36 ± 0.05 mg g^{-1} glass beads to 0.56 ± 0.05 mg g^{-1} glass beads. At the same time, the hydrodynamic diameter of the nanoparticles increased from 119.47 ± 2.28 nm to 187.77 ± 3.35 nm. This may be because that the degree of polymerization was increased with longer exposure time, which in turn helped to produce larger nanoparticles, resulting in higher yields. SEM analysis of the synthesized histamine nanoMIPs was conducted. The image showed that the nanoparticles were quite homogenous in size (Fig. 3). Based on the SEM image scale, histamine nanoMIPs exhibited a dry size of 99–113 nm, which was smaller than that measured by DLS. This could be due to the fact that the nanoparticles shrank upon drying.

Table 1 Yield, size and K_D of histamine nanoMIPs synthesized under different UV exposure times

Exposure time (s)	Yield (particle mass per g of glass beads, mg)	Size (nm)	K_D (nM)
10	0.36 ± 0.05	119.47 ± 2.28	11.30
20	0.45 ± 0.04	156.00 ± 2.69	8.01
30	0.56 ± 0.05	187.77 ± 3.35	0.89

The SPR sensorgram (Fig. 4) showed that the exposure time of 30 second gave the lowest value of apparent dissociation constant K_D, which was 0.89 nM (Table 1). The reason could be that longer exposure time led to the formation of sufficiently rigid nanoparticles with well-formed recognition cavities, which allowed for stronger interactions between the immobilized template and the nanoMIPs.

Basozabal *et al.*[30] utilized a similar approach to synthesize histamine nanoMIPs. The polymerization mixture was initiated using 2.5 min of UV exposure time. With this condition, the nanoparticles with the average hydrodynamic radius of 218.8 nm and the yield of 0.56 mg per gram of glass beads were

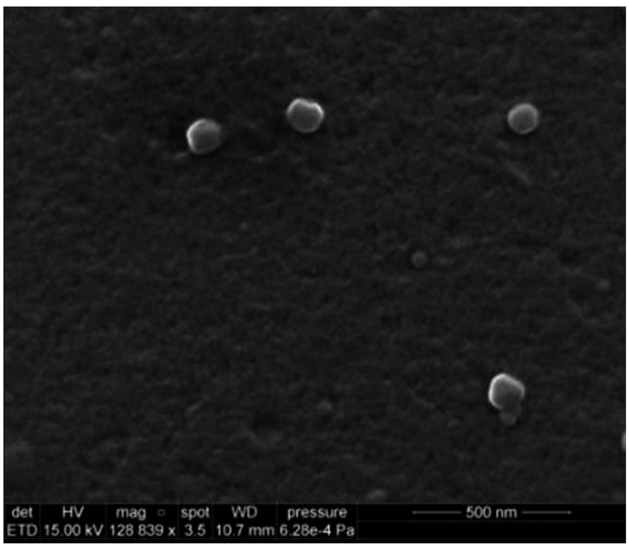

Fig. 3 SEM image of the histamine nanoMIPs.

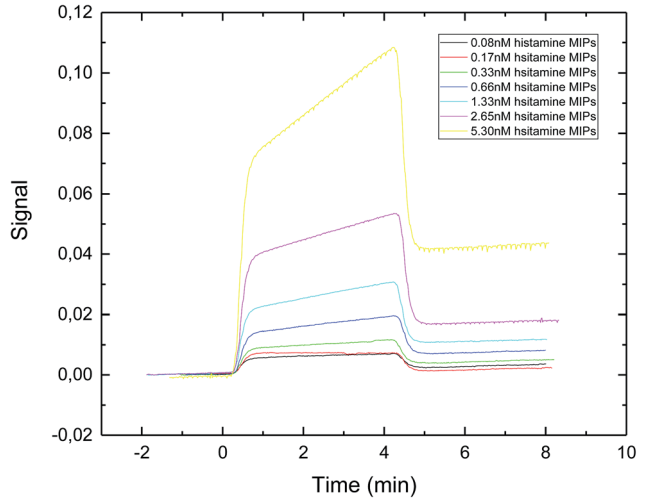

Fig. 4 SPR sensorgram of nanoMIPs injected onto a specific histamine-coated sensor surface. The nanoMIPs were synthesized under UV exposure time of 30 s.

obtained. It is worth to point out that due to the higher power output of our photoreactor, much shorter exposure time was adequate for the synthesis of the nanoMIPs. The apparent K_D reported by Basozabol *et al.*[30] was 0.099 nM while the apparent binding affinity in the current study was 0.890 nM. The difference in reported binding affinity were due to systematic errors in different SPR instrumentation, as well as the fact that we used an online amine coupling procedure whereas the chips prepared in the previous study were prepared offline using glutaraldehyde based conjugation. As such, in this study we were able to subtract the reference signal from the analyte signal.

Based on these results, histamine nanoMIPs with the highest binding affinity were synthesized using the exposure time of 30 second, and this exposure time was chosen for all further experiments. The main drawbacks of solid phase synthesis are low yield and typically there is only one binding site in each nanoparticle. This may result in low binding capacity, which may not suitable for sample preparation applications. However, the high-affinity (K_D = 0.89 nM) of nanoMIPs and small size (~200 nm) make them appropriate for use as receptors in biosensors. Moreover, the product yields can be increased by optimizing the morphology of the solid substrate, such as using high surface-to-volume supporting material as an alternative.

3.2. Selectivity of histamine nanoMIPs

Histamine nanoMIPs were synthesized using MAA as functional monomer. In organic solution, it can form strong hydrogen bond interactions with the nitrogen in the imidazole ring of histamine. When recognition occurred in aqueous solution, hydrogen bond interactions might still be involved to some extent, but it was found that electrostatic interactions served as the main channel to the recognition mechanism.[19] In order to monitor the level of histamine in food samples, all selectivity experiments were conducted in aqueous PBS solution.

To study the selectivity of histamine nanoMIPs, histidine and melamine were selected as an appropriate control. In solid-phase imprinting, non-imprinted polymers cannot be formed on the solid support, as they are immediately removed in the low temperature elution step. Furthermore, it is impractical to extract small fractions of non-imprinted polymer nanoparticles from high concentrations of residual monomers and oligomeric materials. Therefore, it is not possible to produce non-imprinted polymer as a control in this case.

Fig. 5a shows the structures of the three compounds. Histamine can be formed by decarboxylation of histidine. Fig. 5b showed the uptake concentrations of histamine, histidine and melamine by the nanoMIPs under the different concentrations. The results demonstrated that the nanoMIPs had higher (at least 2 fold) binding efficiency towards histamine than its structural analogs. Therefore, it can be concluded that the nanoMIP was selective for histamine.

3.3. OPA fluorometric assay for histamine

An OPA fluorometric assay was developed by using histamine nanoMIPs as artificial antibody. The histamine nanoMIPs were immobilized on the well plate by evaporation overnight. The physically adsorbed nanoMIPs were tightly bound to the surface of the plate and remained on the wells even after several washes with PBS buffer. As each well only required 100 μg nanoMIPs, histamine nanoMIPs obtained from one batch is sufficient for 50 reactions.

OPA is a commonly used reagent which allows for the fluorescent detection and quantification of the primary amine in alkaline conditions, but this simple conjugation has not been used for MIP-based bioassays. In our method, histamine was firstly bound to the nanoMIPs, then OPA was added to form conjugation with the primary amine group of the histamine. The fluorescence signal clearly indicated that the histamine-nanoMIPs complex could be directly detected using the OPA conjugation. On the basis of this method, calibration curves were built as shown in Fig. 6. A good linear correlation between fluorescent intensity and histamine concentration was observed within the range of 1.80–44.98 μM.

Different incubation times were also tested (5 min, 10 min, 30 min, 1 h, 2 h, 4 h and overnight) in order to investigate the possibility of reducing the incubation time. The kinetic binding plot (Fig. 7) showed that the point of saturation was reached after 4 hours. Therefore, 4 hours of incubation time was chosen for all future experiments.

Compared to the "pseudo-ELISA", the process of OPA fluorometric assay was greatly simplified. "Pseudo-ELISA" needed preparation of horseradish peroxidase (HRP) conjugated target solution, as well as long development steps,[25] whereas the OPA fluorometric assay required no pre-conjugation and only took 4 min to give fluorescent signals. Additionally, since there was no enzyme involved, the cost of analysis was significantly reduced.

3.4. Determination of histamine in milk

To test the feasibility of our method to detect histamine in food samples, histamine was spiked into milk with different

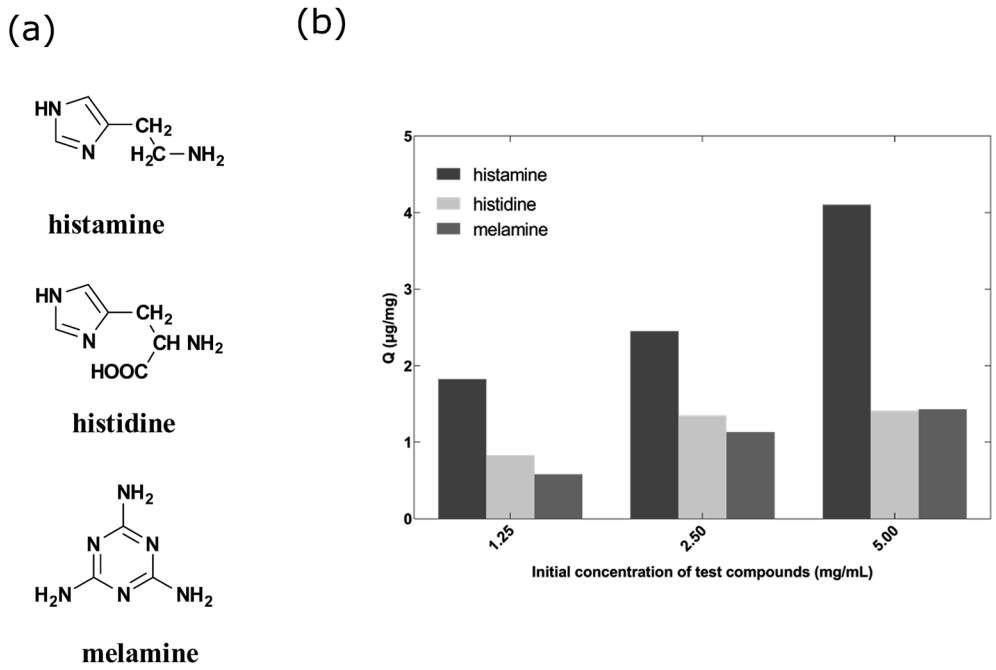

Fig. 5 (a) Chemical structures of histamine, histidine and melamine. (b) Uptake of histamine, histidine and melamine at different concentrations by histamine nanoMIPs (5 mg) in 1 mL PBS buffer.

concentrations (*e.g.* 0 μM, 4.5 μM, 13.5 μM, 27 μM and 40.48 μM). The concentrations of the spiked samples were then determined by interpolating the measured fluorescence intensity using the linear calibration plot. The results showed that the recovery rates of histamine in the spiked samples were in the range of 87.95–101.01% (Table 2). The RSD ($n = 2$) values were in the range of 3.13–7.70%. The limit of the detection was 1.8 μM (0.2 mg L^{-1}), better than SERS- and UV-vis spectrometry-based methods, though not as low as voltammetry-based detection (Table 3). The sensitivity of our approach was much beyond the MRL of histamine in beverages (about 2–20 mg L^{-1}).[5] Furthermore, the recovery rate for non-spiked milk sample was nearly zero, suggesting that the matrix effects from the milk proteins and fats had no interferences on the analytical results. Therefore, this method could eliminate the need of sophisticated sample preparation.

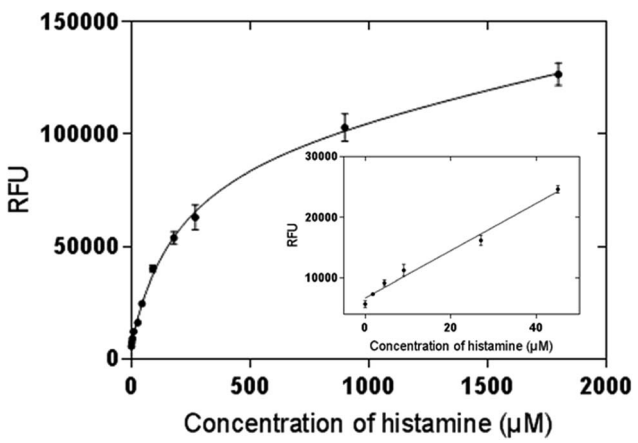

Fig. 6 Saturation curve and calibration curve of histamine nanoMIP-based OPA fluorometric assay. Error bars were for experiments performed in duplicates. The R^2 value of calibration curve was 0.992.

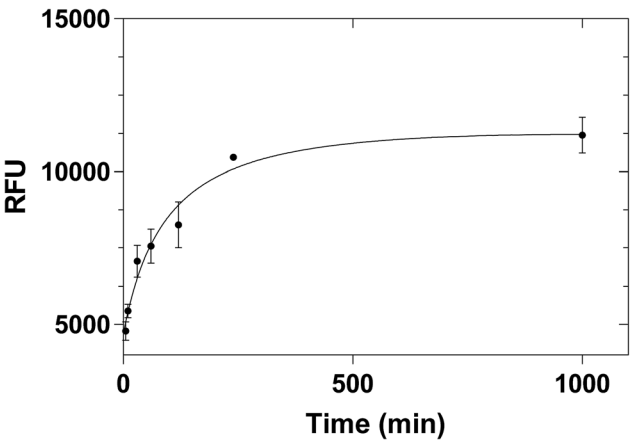

Fig. 7 Equilibrium binding of 2 μg mL^{-1} histamine to 100 μg histamine nanoMIPs. Error bars were for experiments performed in duplicates.

Table 2 Recoveries of histamine from spiked milk samples. The experiments were performed in duplicates

Spiked (μM)	Found (μM)	Recovery (%)
40.48	38.24 ± 3.12	94.45 ± 7.70
27.00	23.755 ± 2.23	87.95 ± 8.27
13.50	12.175 ± 0.54	90.15 ± 4.03
4.50	4.935 ± 0.42	101.01 ± 3.13
0	−1.42 ± 1.48	NA

Table 3 Comparison of this work with previously reported histamine detection methods

Method	Detection limit (mol L^{-1})	Reference
SERS	2.7×10^{-5}	17
Voltammetry	7.4×10^{-11}	18
UV-vis spectrometry	8.05×10^{-5}	19
OPA fluorometric assay	1.8×10^{-6}	This method

4. Conclusions

In conclusion, histamine nanoMIPs were successfully synthesized and characterized using solid-phase synthesis approach. The synthesized histamine nanoMIPs showed high binding affinity and high selectivity towards histamine. The nanoMIP-based fluorometric assay was developed in a microplate format. OPA was used to label the histamine, which enabled histamine to be quantified based on the fluorescent intensity. The assay has been employed to detect histamine in diary milk with detection limit of 1.8 μM and recovery efficiency of more than 85%. The simple, robust and cost-effective assay is very promising for routine high-throughput screening of histamine in complex food matrices.

Conflicts of interest

The authors declare no competing financial interest.

Acknowledgements

This work was financially supported by the Villum Fonden, Denmark, Project No. 13153.

References

1 I. San Mauro Martin, S. Brachero and E. Garicano Vilar, *Allergol. Immunopathol.*, 2016, **44**, 475–483.
2 R. Leurs, P. L. Chazot, F. C. Shenton, H. D. Lim and I. J. De Esch, *Br. J. Pharmacol.*, 2009, **157**, 14–23.
3 L. Maintz and N. Novak, *Am. J. Clin. Nutr.*, 2014, **85**, 832–833.
4 S. Wöhrl, W. Hemmer, M. Focke, K. Rappersberger and R. Jarisch, *Allergy Asthma Proc.*, 2004, **25**, 305–311.
5 T. Tang, K. Qian, T. Shi, F. Wang, J. Li, Y. Cao and Q. Hu, *Food Control*, 2011, **22**, 1203–1208.
6 M. J. R. Nout, *Food Res. Int.*, 1994, **27**, 291–298.
7 C. A. L. De La Torre, *Braz. J. Vet. Res. Anim. Sci.*, 2013, **50**, 430.
8 B. S. Hwang, J. T. Wang and Y. M. Choong, *Food Chem.*, 2003, **82**, 329–334.
9 T. Yoshitake, F. Ichinose, H. Yoshida, K. I. Todoroki, J. Kehr, O. Inoue, H. Nohta and M. Yamaguchi, *Biomed. Chromatogr.*, 2003, **17**, 509–516.
10 L. Y. Zhang and M. X. Sun, *J. Chromatogr. A*, 2004, **1040**, 133–140.
11 P. Q. Leng, F. L. Zhao, B. C. Yin and B. C. Ye, *Chem. Commun.*, 2015, **51**, 8712–8714.
12 A. Marcobal, M. C. Polo, P. J. Martín-Álvarez and M. V. Moreno-Arribas, *Food Res. Int.*, 2005, **38**, 387–394.
13 J. Wackerlig and R. Schirhagl, *Anal. Chem.*, 2016, **88**, 250–261.
14 L. Figueiredo, G. L. Erny, L. Santos and A. Alves, *Talanta*, 2016, **146**, 754–765.
15 L. Uzun and A. P. F. Turner, *Biosens. Bioelectron.*, 2016, **76**, 131–144.
16 J. Ashley, M.-A. Shahbazi, K. Kant, V. A. Chidambara, A. Wolff, D. D. Bang and Y. Sun, *Biosens. Bioelectron.*, 2017, **91**, 606–615.
17 F. Gao, E. Grant and X. Lu, *Anal. Chim. Acta*, 2015, **901**, 68–75.
18 M. Akhoundian, A. Rüter and S. Shinde, *Sensors*, 2017, **17**, 645.
19 F. A. Trikka, K. Yoshimatsu, L. Ye and D. A. Kyriakidis, *Amino Acids*, 2012, **43**, 2113–2124.
20 N. Pérez-Moral and A. G. Mayes, *Anal. Chim. Acta*, 2004, **504**, 15–21.
21 C. He, Y. Long, J. Pan, K. Li and F. Liu, *J. Biochem. Biophys. Methods*, 2007, **70**, 133–150.
22 F. Canfarotta, A. Poma, A. Guerreiro and S. Piletsky, *Nat. Protoc.*, 2016, **11**, 443.
23 J. Czulak, A. Guerreiro, K. Metran, F. Canfarotta, A. Goddard, R. H. Cowan, A. W. Trochimczuk and S. Piletsky, *Nanoscale*, 2016, **8**, 11060–11066.
24 Y. Garcia, K. S. Kempisty, E. Pereira, E. Piletska and S. Piletsky, *Anal. Methods*, 2017, **9**, 4592–4598.
25 S. Tang, F. Canfarotta, K. Smolinska-kempisty, E. Piletska, S. Piletsky and A. Guerreiroc, *Anal. Methods*, 2017, **9**, 2853–2858.
26 K. Smolinska-Kempisty, A. Guerreiro, F. Canfarotta, C. Cáceres, M. J. Whitcombe and S. Piletsky, *Sci. Rep.*, 2016, **6**, 37638.
27 C. C. Huang and W. L. Tseng, *Analyst*, 2009, **134**, 1699–1705.
28 Y. Hoshino, T. Kodama, Y. Okahata and K. J. Shea, *J. Am. Chem. Soc.*, 2008, **130**, 15242–15243.
29 E. V. Piletska, A. R. Guerreiro, M. J. Whitcombe and S. A. Piletsky, *Macromolecules*, 2009, **42**, 4921–4928.
30 I. Basozabal, A. Guerreiro, A. Gomez-Caballero, M. Aranzazu Goicolea and R. J. Barrio, *Biosens. Bioelectron.*, 2014, **58**, 138–144.

